Thermoelectric Effects in Nanowire-Based MOSFETs

R. Bosisio[1], G. Fleury[1], C. Gorini[2], and J.-L. Pichard[*1]

[1]SPEC, CEA, CNRS, Université Paris-Saclay, CEA-Saclay, 91191 Gif-sur-Yvette, France
[2]Institut für Theoretische Physik, Universität Regensburg, 93040 Regensburg, Germany

Abstract

We review a series of works describing thermoelectric effects in gated disordered nanowires (field effect transistor device configuration). After considering the elastic coherent regime characterizing sub-Kelvin temperatures, we study the inelastic activated regime occurring at higher temperatures, where electronic transport is dominated by phonon-assisted hops between localised states (Mott variable range hopping). The thermoelectric effects are studied as a function of the location of the Fermi level inside the nanowire conduction band, notably around its edges where they become very large. We underline the interest of using electron-phonon coupling around the band edges of large arrays of parallel nanowires for energy harvesting and hot spot cooling at small scales. Multiterminal thermoelectric transport and ratchet effects are eventually considered in the activated regime.

PACS numbers: 79.10.N- Thermoelectronic phenomena, 72.20.Ee Hopping transport, 62.23.Hj Nanowires, 85.30.Tv Field effect transistors, 72.20.Pa Thermoelectric effects in semiconductors and insulators

Keywords: Disordered gated nanowires, Elastic and Activated thermoelectric transport, Energy harvesting and heat management at submicron scales, Thermoelectric ratchets

1 Introduction

Let us consider a nanowire (NW) connecting two electron reservoirs. If one imposes a temperature difference δT between the reservoirs, this induces an electrical current I_e which can be suppressed by a voltage difference $-\delta V$. The ratio $S = -(\delta V/\delta T)_{I_e=0}$ defines the NW Seebeck coefficient (or thermopower). If one imposes a voltage difference δV when $\delta T = 0$, this induces electrical and heat currents I_e and I_Q. The ratio $\Pi = I_Q/I_e$ defines the NW Peltier coefficient. In the linear response regime, the Peltier and Seebeck coefficients are related via the Kelvin-Onsager relation $\Pi = ST$.

Either a temperature gradient across a NW can produce electricity (Seebeck effect), or an electric current through the same NW can create a temperature difference between its two sides (Peltier effect). These thermoelectric effects (TEs) can be used either for harvesting electrical energy from wasted heat or for cooling things. Today, the batteries of our cell phones and laptops need to be charged too often. Tomorrow, the Seebeck effect could allow us to exploit the wasted heat to produce a part of the electrical energy necessary for many devices used for the internet of things. Another important issue is cooling, notably the hot spots in microprocessors. The last decades have been characterized by an exponential growth of the on-chip power densities. Values of the order of $100W/cm^2$ have become common [1]. More than our ability to reduce their sizes, the limitation of the performances of microprocessors comes from the difficulty of managing heat in ever-smaller integrated circuits. Improving Peltier cooling and heat management from

*Corresponding author. Email: jean-louis.pichard@cea.fr

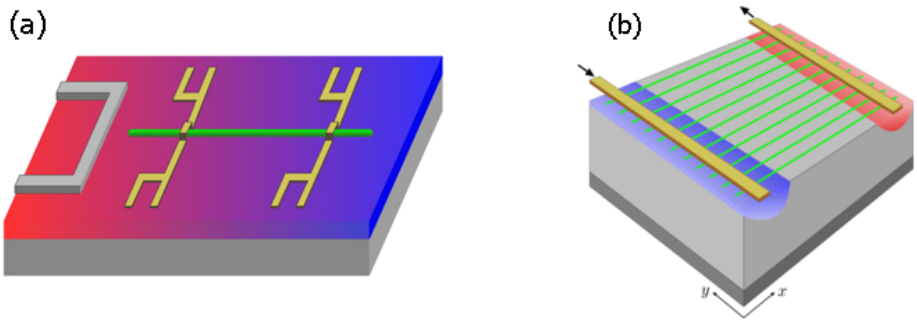

Figure 1: *NW-based MOSFETs: (**a**) A single NW (green) is deposited on an insulating substrate (red and blue). The source and the drain are made of two metallic electrodes (yellow), while Joule heating from an extra electrode (left side) can induce a temperature difference between the NW extremities. Varying the voltage V_g applied upon the back gate (grey), one can shift the NW conduction band and probe thermoelectric transport in the bulk of the band, around its edges or even outside the band. This setup has been used in Ref. [7] for measuring the thermopower $\mathcal{S}$ of individual Si and Ge/Si NWs as a function of V_g at room temperature. (**b**) Array of parallel NWs deposited on a substrate with a back gate. The blue and red spots illustrate local cooling and heating effects in the activated regime, discussed in Sec.4.*

the nanoscale (e.g. molecules) to the microscale (e.g. quantum dots and nanowire arrays) is thus of paramount importance to boost microprocessors' performance.

In a typical two-terminal configuration in which a device is coupled to two electronic reservoirs held at different temperatures, the ratio η of the output power over the heat extracted from the hot reservoir measures the efficiency of the heat-to-work thermoelectric conversion. It cannot exceed the Carnot efficiency $\eta_C = 1 - T_C/T_H$, where T_C (T_H) is the temperature of the cold (hot) reservoir. The figure of merit ZT gives the maximal efficiency η_{max} in terms of the Carnot limit [2, 3].

$$ZT = \frac{GS^2}{K^e + K^{ph}}T; \qquad \eta_{max} = \eta_C \frac{\sqrt{ZT+1}-1}{\sqrt{ZT+1}+1}, \tag{1}$$

where G is the electrical conductance, while K^e and K^{ph} are respectively the electronic and phononic parts of the thermal conductance. The larger ZT, the better the efficiency. A high efficiency is however mainly useful if coupled with good electrical output power, measured by the power factor $Q = GS^2$. Maximising both ZT and Q is the central challenge of (linear response) thermoelectricity. This is not easy since G, K_e, K_{ph} and S are not independent.

The interest of NWs for thermoelectric conversion was pointed out in Ref. [4]. Taking arrays of parallel doped Si NWs of 50 nm in diameter yields $ZT = 0.6$ at room temperature, a much larger value than in bulk silicon. This was attributed to a 100-fold reduction in thermal conductivity, assuming than S and G keep the same values than in doped bulk Si. Using standard Si-based semi-conductor technology for thermoelectric conversion looks very interesting: In contrast to used thermoelectric materials, Si is cheap and non toxic, and NW-based one dimensional (1D) electronics is a well developed technology. Moreover, one can use metallic gates for tuning the NW electron density, in the field effect transistor (FET) device configuration. A detailed experimental study of electron tunneling and interferences in 1D Si-doped Ga-As MOSFETs can be found in Ref. [5], where the electrical conductance $G(E)$ of $1\mu m$ long NWs at $35mK$ is given as a function of the gate voltage V_g. One can make [6] arrays of vertical NW-based FET, each of them having a uniform wrap-around gate. To grow millions of thin NWs per cm^2 is possible. This gave us the motivation to study the TEs in 1D MOSFETs, from cryogenic temperatures where electron transport remains coherent towards higher temperatures where transport becomes activated, as a function of the location of the Fermi potential E_F inside the NW conduction band. The considered setups are sketched in Fig. 1.

2 Elastic thermoelectric transport

To model a gated NW, we have considered in Ref. [8] a chain of N sites coupled to two electronic reservoirs L (left) and R (right), in equilibrium at temperature $T_L = T + \delta T$ [$T_R = T$] and chemical potential $\mu_L = E_F + \delta\mu$ [$\mu_R = E_F$]. The Hamiltonian of the chain reads

$$\mathcal{H} = -t \sum_{i=1}^{N-1} \left(c_i^\dagger c_{i+1} + \text{h.c.} \right) + \sum_{i=1}^{N} (\epsilon_i + V_g) c_i^\dagger c_i \,, \tag{2}$$

where $c_i^\dagger$ and c_i are the creation and annihilation operators of one electron on site i and t is the hopping energy. The lattice spacing $a = 1$, the ϵ_i are (uncorrelated) random numbers uniformly distributed in the interval $[-W/2, W/2]$. $\sum_i V_g c_i^\dagger c_i$ describes the effect of an external gate. Varying V_g, one can probe thermoelectric transport either in the bulk of the NW conduction band, around its edges or even outside the band.

2.1 Typical thermopower

For the Hamiltonian (2), the localisation length $\xi(E)$ and the density of states (DOS) $\nu(E)$ per site are analytically known [9] in the weak disorder limit $W \leq t$. Within the band ($|E - V_g| \lesssim 1.5t$), $\xi(E)^{-1}$ can be expanded in integer powers of W while $\nu(E)$ remains well described by the DOS of the clean chain ($W = 0$). This gives the bulk expressions

$$\xi_b(E) \approx \frac{24}{W^2} \left(4t^2 - |E - V_g|^2 \right) , \qquad \nu_b(E) \approx \frac{1}{2\pi t \sqrt{1 - (|E - V_g|/2t)^2}} . \tag{3}$$

When $E - V_g$ approaches the band edges $\pm 2t$, these expressions lead to divergences of ν and ξ^{-1}. As shown by Derrida and Gardner, these divergences are spurious and the correct expressions near the edges become

$$\xi_e(E) = 2 \left(\frac{12t^2}{W^2} \right)^{1/3} \frac{\mathcal{I}_{-1}(X)}{\mathcal{I}_1(X)} \tag{4}$$

$$\nu_e(E) = \sqrt{\frac{2}{\pi}} \left(\frac{12}{tW^2} \right)^{1/3} \frac{\mathcal{I}_1(X)}{[\mathcal{I}_{-1}(X)]^2} \tag{5}$$

where

$$X = (|E - V_g| - 2t) t^{1/3} (\frac{12}{W^2})^{2/3}, \qquad \mathcal{I}_n(X) = \int_0^\infty y^{n/2} \, e^{-\frac{1}{6}y^3 + 2Xy} \, dy \,. \tag{6}$$

The typical transmission coefficient $\mathcal{T}(E)$ of the disordered chain behaves as $\exp -2N/\xi(E)$ while the electrical conductance $G \approx \frac{2e^2}{h} \mathcal{T}(E_F)$ in the limit $T \to 0$. Using Cutler-Mott formula,

$$S = \frac{\pi^2 k_B^2 T}{3|e|t} \mathcal{S} \quad \text{with} \quad \mathcal{S} \approx -t \left. \frac{\mathrm{d} \ln \mathcal{T}}{\mathrm{d}E} \right|_{E_F} , \tag{7}$$

one can obtain the typical thermopower S_0 from the weak disorder expansions of $\xi(E)$. This gives respectively in the bulk of the band and at its edges:

$$\mathcal{S}_0^b = N \frac{(E_F - V_g) \, W^2}{96 t^3 [1 - ((E_F - V_g)/2t)^2]^2} , \tag{8}$$

$$\mathcal{S}_0^e = 2N \left(\frac{12t^2}{W^2} \right)^{1/3} \left\{ \frac{\mathcal{I}_3(X)}{\mathcal{I}_{-1}(X)} - \left[\frac{\mathcal{I}_1(X)}{\mathcal{I}_{-1}(X)} \right]^2 \right\} , \tag{9}$$

where $X = X(E = E_F)$. Outside the band, the disorder effect becomes negligible and one obtains

$$\frac{\mathcal{S}_0^{TB}}{N} \underset{N \to \infty}{\approx} -\frac{1}{N} \frac{2t}{\Gamma(E_F)} \left. \frac{\mathrm{d}\Gamma}{\mathrm{d}E} \right|_{E_F} \mp \frac{1}{\sqrt{\left(\frac{E_F - V_g}{2t} \right)^2 - 1}} \tag{10}$$

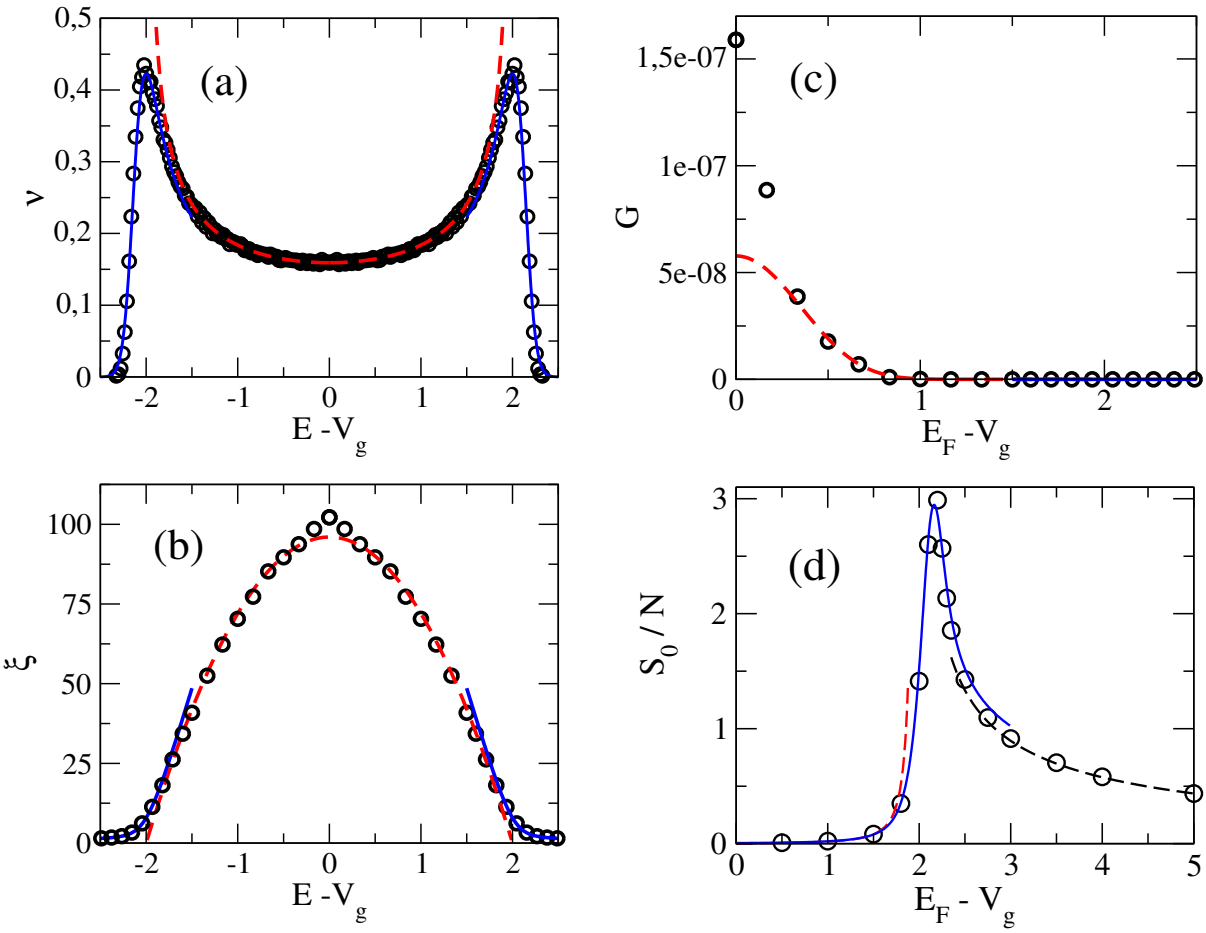

Figure 2: *1D Anderson model with $W = t = 1$: (**a**) Density of states per site $\nu(E)$, (**b**) localisation length $\xi(E)$, (**c**) typical conductance G (in units of $2e^2/h$) and (**d**) typical thermopower S_0 (in units of $(\pi^2 k_B)/(3e)\, k_B T$). In all panels, the red dashed line and the blue continuous line give the weak disorder behaviours in the bulk and near the edges (Eqs. (3-5) and Eqs. (8-9)), while the black dashed line in (d) corresponds to Eq.* (10)*. Circles are numerical results obtained for $N = 1600$ ((a) and (b)) and $N = 800$ ((c) and (d)).*

with a + sign when $E_F \leq V_g - 2t$ and a − sign when $E_F \geq V_g + 2t$. In Fig. 2, one can see that the analytical weak disorder expressions of the DOS per site $\nu(E)$, of the localisation length $\xi(E)$, of the electrical conductance $G(E)$ and of the typical thermopower $S_0(E)$ describe accurately numerical results (for more details, see Ref. [8]), even if they are calculated for a relatively large disorder ($W = t$).

2.2 Mesoscopic Fluctuations

In the elastic regime, the sample-to-sample fluctuations of the dimensionless thermopower $\mathcal{S}$ around its typical values $\mathcal{S}_0^b$ or $\mathcal{S}_0^e$ are very large. If $E_F = V_g$, $\mathcal{S}_0 = 0$ due to particle-hole symmetry but the mesoscopic fluctuations allow for a large $\mathcal{S}$ anyway. Assuming Poisson statistics for the energy levels, Van Langen *et al* showed in Ref. [10] that the thermopower distribution is a Lorentzian when $N \gg \xi$,

$$P(\mathcal{S}) = \frac{1}{\pi} \frac{\Lambda}{\Lambda^2 + (\mathcal{S} - \mathcal{S}_0)^2} \,. \tag{11}$$

The width $\Lambda = 2\pi t/\Delta_F$ is given by the mean level spacing $\Delta_F = 1/(N\nu(E_F))$ at the Fermi energy E_F. Van Langen *et al* assumed $\mathcal{S}_0 = 0$, an assumption which is only correct at the band centre. We have calculated $P(\mathcal{S})$ using recursive Green function method for different values of V_g and have numerically checked [8] that Eq. (11) describes also $P(\mathcal{S})$ if one takes for $\mathcal{S}_0$ the value given by Eqs. (8) or (9) instead of $\mathcal{S}_0 = 0$. As one crosses the band edges, we have numerically observed a sharp crossover towards a Gaussian distribution

$$P(\mathcal{S}) = \frac{1}{\sqrt{2\pi}\lambda} \exp\left[-\frac{(\mathcal{S} - \mathcal{S}_0)^2}{2\lambda^2}\right] , \tag{12}$$

where the typical value $\mathcal{S}_0$ is given by Eq. (10) and the width λ increases linearly with $\sqrt{N}$ and W. In Ref. [8], one can find numerical results which are perfectly described by the above analytical expressions when $W = t$.

3 Inelastic thermoelectric transport

When one increases the temperature T, electron transport becomes mainly inelastic and activated. The inelastic effects can be due to electron-electron, electron-photon and electron-phonon interactions. In Ref. [11], we have studied the Variable Range Hopping (VRH) regime introduced by Mott [12] where electron-phonon coupling dominates. Fig.3 (a) illustrates how electrons propagate through the NW in the VRH regime.

3.1 Variable Range Hopping

In the VRH regime, the electrons propagate by hopping from one localised state to another, of higher energy by absorbing a phonon or of lower energy by emitting a phonon. Let us summarize Mott's original argument [12]. The electron transfer from a state i to another state j separated by a distance L_{ij} in space and Δ_{ij} in energy results from a competition between the probability $\propto \exp -(L_{ij}/\xi)$ to tunnel over a length L_{ij} and the probability $\propto \exp -\Delta_{ij}/(k_B T)$ to change the electron energy by an amount Δ_{ij} , where ν is the DOS per site. These estimates neglect the energy dependence of ξ and ν around E_F. In 1D, the optimal hopping length is given by the *Mott length* $L_M \simeq (\xi/2\nu k_B T)^{1/2}$, if the localisation lengths $\xi_{i,j}$ and DOS per unit length $\nu(E_{i,j})$ do not vary within the Mott energy window $\Delta_M = 1/(\nu L_M) = k_B\sqrt{TT_M}$ around E_F. L_M decreases as the temperature increases. One defines the activation temperature $k_B T_x \simeq \xi/(2\nu L^2)$ at which $L_M \simeq L$ and the Mott temperature $k_B T_M \simeq 2/(\nu\xi)$ at which $L_M \simeq \xi$. The inelastic VRH regime corresponds to $T_x < T < T_M$ where the electrical conductance

$$G \propto \exp -(2L_M/\xi) \propto \exp -(\Delta_M/k_B T). \tag{13}$$

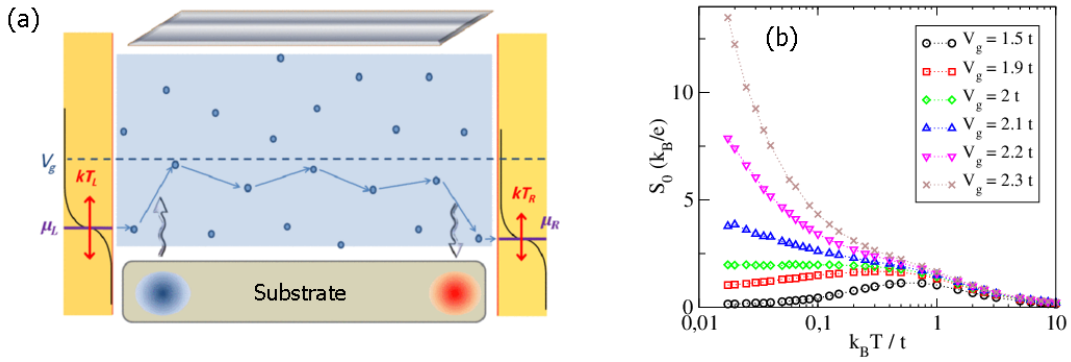

Figure 3: ***(a)*** *The electronic localised states (blue dots) are randomly located along the chain within an energy band of width* $4t+W$ *(shaded light blue region). In the left and right reservoirs, the electrons are at equilibrium with Fermi-Dirac distributions of temperatures* $T_L = T + \delta T$, $T_R = T$ *and electrochemical potentials* $\mu_L = E_F + \delta\mu$, $\mu_R = E_F$. *Varying the voltage* V_g *applied to the gate (top grey region) shifts the NW conduction band, making possible to probe electron transport inside the band, around its edges or outside the band. The electrons can hop between states of different energies by absorbing or emitting a phonon. For a NW deposited on a substrate, the phonons are provided by the substrate and characterized by a Bose-Einstein distribution of temperature* T_S *(*$T_S = T$ *throughout the paper, except in Sec.5). Electrons injected near the lower band edge mainly find available states to jump to at higher energies near the source (left reservoir). This implies that the phonons are mainly absorbed from the substrate near the source (blue region), and emitted back to the substrate near the drain (red region), as indicated by the two arrows.* ***(b)*** *Typical thermopower* S_0 *(in units of* k_B/e*) as a function of* k_BT/t, *calculated for a chain of length* $L = 200$ *(*$E_F = 0$ *and* $W = t$*) for increasing values of* V_g.

Below T_x elastic tunneling dominates, while above T_M $L_M < \xi$ and transport becomes simply activated. In 1D, the crossover from VRH to simply activated transport takes even place [13, 14] at a temperature T_a lower than T_M. The reason is the presence of highly resistive regions in energy-position space, where 1D electrons cannot find empty states at distances $\sim \Delta_M, L_M$.

3.2 Random Resistor Network with energy-dependent localisation length and density of states

If the variation of $\xi(E)$ and $\nu(E)$ as a function of the energy E is not negligible within the characteristic scale Δ_M, we need to go beyond this simple argument, notably around the 1D band edges. We use a simplified model where the E_i are N uncorrelated variables of probability given by the DOS $\nu(E)$ of the 1D Anderson model for a chain of length $L = Na$ $(a = 1)$, while the N localisation lengths $\xi(E_i)$ are given by the typical values of this model (Eqs. (3) and (4)). The N positions x_i are taken at random in the interval $[0, L]$. As in Refs. [15, 16], we solve the corresponding Miller-Abrahams random resistor network [17] (RRN) made of all possible links connecting the N nodes given by the N localised states. Each pair of nodes i, j is connected by an effective resistor, which depends on the transition rates Γ_{ij}, Γ_{ji} induced by local electron-phonon interactions. For a pair of localised states i and j of energies E_i and E_j, Fermi golden rule [16] gives:

$$\Gamma_{ij} = \gamma_{ij}\, f_i\, (1 - f_j)\, [N_{ij} + \theta(E_i - E_j)] \;, \tag{14}$$

where f_i is the occupation number of state i and $N_{ij} = [\exp\{|E_j - E_i|/k_BT\} - 1]^{-1}$ is the phonon Bose distribution at energy $|E_j - E_i|$. The Heaviside function accounts for the difference between phonon absorption and emission [18]. γ_{ij} is the hopping probability $i \to j$ due to the absorption/emission of a phonon when i is occupied and j is empty. It is given by

$$\frac{\gamma_{ij}\,(1/\xi_i - 1/\xi_j)^2}{\gamma_{ep}} = \left[\frac{\exp\{-2x_{ij}/\xi_j\}}{\xi_i^2} + \frac{\exp\{-2x_{ij}/\xi_i\}}{\xi_j^2} - \frac{2\exp\{-x_{ij}(1/\xi_i + 1/\xi_j)}{\xi_i\xi_j}\right] \tag{15}$$

where $x_{ij} = |x_i - x_j|$ and γ_{ep} depends on the electron-phonon coupling strength and of the phonon density of states. If the energy dependence of ξ and ν can be neglected within Δ_M, one recovers the usual limit $\gamma_{ij} \simeq \gamma_{ep} \exp(-2x_{ij}/\xi)$.

The direct transition rates between each state i and the contacts α (source $\alpha = L$ and drain $\alpha = R$) are assumed do be dominated by elastic tunneling (see Refs. [15, 16]) and read

$$\Gamma_{i\alpha} = \gamma_{e,\alpha} \exp(-2x_{i\alpha}/\xi_i)\, f_i\, [1 - f_\alpha(E_i)]\,. \tag{16}$$

$f_\alpha(E) = [\exp\{(E-\mu_\alpha)/k_BT\}+1]^{-1}$ is the contact α's Fermi-Dirac distribution, $x_{i\alpha}$ denotes the distance of the state i from α, and $\gamma_{e,\alpha}$ is a rate quantifying the coupling between the localized states and the contact α. The electric currents flowing between each pair of states and between states and contacts read

$$I_{ij} = e\,(\Gamma_{ij} - \Gamma_{ji}), \tag{17a}$$

$$I_{i\alpha} = e\,(\Gamma_{i\alpha} - \Gamma_{\alpha i}), \qquad \alpha = L, R. \tag{17b}$$

$e < 0$ is the electron charge. Hereafter, we will take $\gamma_{ep} = t/\hbar$ and symmetric couplings $\gamma_{e,L} = \gamma_{e,R} = t/\hbar$.

For solving the RRN, we consider it at equilibrium with a temperature T and a chemical potential $\mu = E_F$ everywhere. A small electric current I_e can be driven by adding to the left contact (the source) a small increase $\delta\mu$ of its chemical potential (Peltier configuration). If $\delta\mu$ is sufficiently small, one has $I_e \propto \delta\mu$ (linear response). At equilibrium ($\delta\mu = 0$), the N occupation numbers f_i are given by Fermi-Dirac distributions $f_i^0 = (\exp(E_i - E_F)/k_BT + 1)^{-1}$. When $\mu_L \to E_F + \delta\mu$, $f_i \to f_i^0 + \delta f_i$. For having the currents I_{ij} and $I_{i\alpha}$, we only need to calculate the N changes δf_i induced by $\delta\mu \neq 0$. Imposing current conservation at each node i of the network ($\sum_j I_{ij} + \sum_\alpha I_{i\alpha} = 0$) and neglecting terms $\propto \delta f_i.\delta f_j$ (linear response), one obtained N coupled linear equations. Solving numerically this set of equations gives the N changes δf_i and hence all the currents I_{ij} and $I_{i\alpha}$. From this, we can calculate the total charge $I_L^e = -\sum_i I_{iL}$ and heat $I_{L(R)}^Q = \sum_i (E_i - \mu_{L(R)})/e) I_{iL(R)}$ currents, and hence the electrical conductance G, the Peltier coefficient Π and the Seebeck coefficient S in the VRH regime.

$$G = \frac{I_L^e}{\delta\mu/e}, \quad \Pi = \frac{I_L^Q}{I_L^e}, \quad S = \frac{1}{T}\frac{I_L^Q}{I_L^e}. \tag{18}$$

In the last equation, the Kelvin-Onsager relation $\Pi = ST$ has been used for obtaining the thermopower S from the Peltier coefficient Π.

3.3 Activated thermoelectric transport in arrays of parallel NWs

Using the 1D weak-disorder expressions (Eqs. (3)-(5)) for $\nu(E)$ and $\xi(E)$, we have studied activated transport through N localised states of energy E_i and localisation length $\xi(E_i)$. The states were assumed to be randomly located along a chain of length $L = Na$, and the energies E_i were taken at random with a probability $\nu(E)$ inside an energy band $[-2\epsilon, 2\epsilon]$ where $\epsilon = t + W/4$. The corresponding thermopower distributions $P(S)$ are given and discussed in Ref. [11]. We reproduce in Fig. 3 (**b**) the curves giving the typical thermopower S_0 (in units of k_B/e) as a function of k_BT/t for increasing values of V_g. Taking $E_F = 0$, S_0 has been calculated for a chain of length $L = 200$ with $W = t$. $V_g = 0$ corresponds to the band centre and $V_g/t = \pm 2.5$ to the band edges. When $k_BT < t$, S_0 remains small within the band ($V_g \approx 1.5t$), but becomes much larger around its edges ($V_g = 2.3t$). At higher temperatures, S_0 decreases and becomes independent of V_g. If activated transport at the band edges give rise to large thermopowers, it is also characterized by small electrical conductances, which defavor large values for the power factors Q. This led us to consider in Ref. [19] arrays of parallel nanowires in the field effect transistor device configuration. In such arrays, the conductances add while the thermopower fluctuations self-average. As estimated in Ref. [19], a large electronic figure of merit $Z_eT \approx 3$

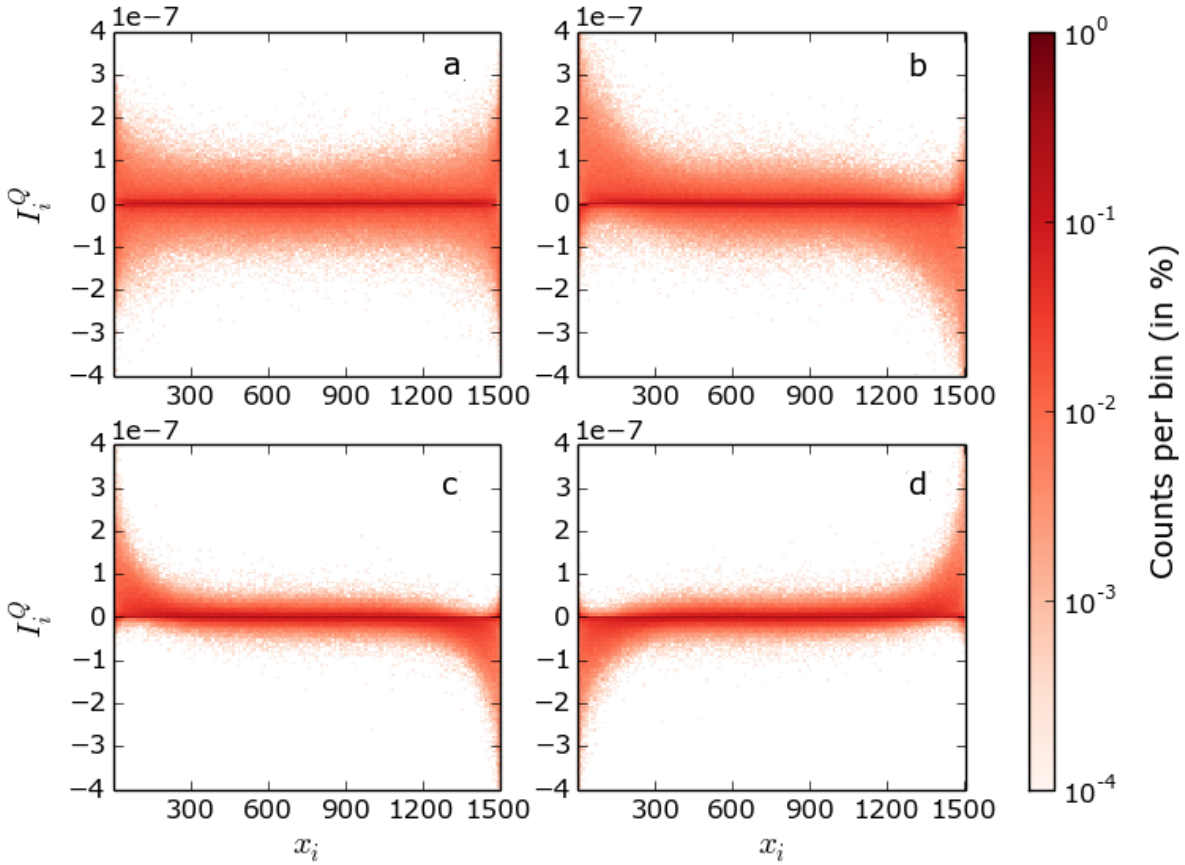

Figure 4: *2D histograms giving the distribution of local heat currents I_i^Q (Eq. (19)) as a function of the position x_i along the NW, for four values of the gate potential: (a) $V_g = 0$, (b) $V_g = t$, (c) $V_g = 2.25t$ and (d) $V_g = -2.25t$. Parameters: $L = 1500$, $W = t$, $k_BT = 0.1t$, $\delta\mu = 10^{-5}t$, statistics over 500 NWs.*

can be reached near the band edges if one neglects the phononic contribution K^{ph} to the thermal conductance, while the maximal output power $P_{max} = Q(\delta T)^2/4$ which can be extracted from $M = 10^5$ parallel silicon NWs can be of the order of $P_{max} \approx 20\tilde{\gamma}_e \mu W$ for $\delta T \approx 10K$ and $T \approx 100K$. Estimates of the constant $\tilde{\gamma}_e = \gamma_e \hbar/t$ give values $\approx 0.01 - 1$. The larger is M or δT, the larger is P_{max}. If one takes into account K^{ph}, we expect that $ZT \approx Z_eT/(1 + 2/\tilde{\gamma}_e)$ for Silicon suspended NWs, while $ZT \approx Z_eT/(1 + 20/\tilde{\gamma}_e)$ for Si NWs deposited on a SiO_2 substrate.

4 Using electron-phonon coupling for managing heat

The phonons have no charge and cannot be manipulated with bias and gate voltages, in contrast to electrons. This makes difficult to manage heat over small scales, unless we take advantage of the electron-phonon coupling for transfering heat from the phonons towards the electrons. Let us show how this can be done using phonon-activated transport near the edges of a NW conduction band. We take a NW deposited on a substrate with a back gate, and assume that the transport of NW-electrons is activated mainly because of the substrate phonons. Let us consider a pair of localised states i and j. The heat current absorbed from (or released to) the substrate phonon bath by an electron hopping from i to j reads $I_{ij}^Q = (E_j - E_i)\, I_{ij}^N$, where $I_{ij}^N = \Gamma_{ij} - \Gamma_{ji}$ is the hopping particle current between i and j. The local heat current associated to the state i is given by summing over the hops from i to all the states j:

$$I_i^Q = \sum_j I_{ij}^Q = \sum_j (E_j - E_i)\, I_{ij}^N. \tag{19}$$

In Fig. 4, we show 2D histograms of the local heat currents I_i^Q as a function of the position x_i of the state i inside the NW. We take the convention that I_i^Q is positive (negative) when the phonons are absorbed (emitted), thus heating (cooling) the electrons at site i. We have numerically solved the random resistor network (see subsection 3.2) for a temperature $k_BT = 0.5t$, $W = t$ and four different values of V_g, corresponding to electron injection at the band center ($V_g = 0$), below the band centre ($V_g = t$) and around the lower ($V_g = 2.25t$) and upper ($V_g = -2.25t$) band edges of the NW conduction band. At the band centre, the fluctuations of the local heat currents are symmetric around a zero average. They are larger near the NW boundaries and remain independent of the coordinate x_i otherwise. Away from the band center, one can see that the fluctuations are no longer symmetric near the NW boundaries, though they become symmetric again far from the boundaries. When the electrons are injected through the NW in the lower energy part of the NW band, more phonons of the substrate are absorbed than emitted near the source electrode. The effect is reversed when the electrons are injected in the higher energy part of the band (by taking a negative gate potential V_g): It is now near the drain that the phonons are mainly absorbed. The 2D histograms corresponding to $V_g = 2.25t$ and $-2.25t$ are symmetric by inversion with respect to $I_i^Q = 0$.

As explained in Refs. [19, 20], activated transport near the band edges of disordered NWs opens interesting ways for managing heat at small scales, notably for cooling hot spots in microprocessors. Taking $M = 2.10^5$ NWs contacting two 1−cm long electrodes, one estimates that we could transfer 0.15 mW from the source side towards the drain side by taking $\delta\mu/e \approx 1\,\mathrm{mV}$ at $T = 77\,\mathrm{K}$. Again, the larger is M or $\delta\mu$, the larger is the heat of the substrate which can be transfered from the source towards the drain by hot electrons.

5 Activated Multi-terminal thermoelectric transport and Ratchet effects

In Secs. 3 and 4, we have discussed activated transport in a configuration where the source, drain and substrate were at the same equilibrium temperature T, the heat and particle currents between the source and the drain being induced by a small voltage bias $\delta\mu$ and/or temperature bias δT. More generally, a disordered NW deposited on a substrate can be viewed as the three-terminal setup sketched in Fig. 5 (**a**): Two electronic reservoirs L (source) and R (drain) at equilibrium with electrochemical potentials μ_L, μ_R, and temperatures T_L, T_R, while the substrate provides a third reservoir S of phonons at a temperature T_S. Heat and particles can be exchanged between L and R, but only heat with S. The particle currents I_L^N, I_R^N, and the heat currents I_L^Q, I_R^Q, I_S^Q are taken positive when they enter the NW from the three reservoirs. The drain is chosen as reference ($\mu_R \equiv E_F$ and $T_R \equiv T$) and we set $\delta\mu = \mu_L - \mu_R$, $\delta T = T_L - T_R$, and $\delta T_S = T_S - T_R$. In linear response the charge and heat currents I_L^N, I_L^Q, and the heat current I_S^Q can be expressed à la Onsager in terms of the corresponding driving forces

$$\begin{pmatrix} I_L^N \\ I_L^Q \\ I_S^Q \end{pmatrix} = \begin{pmatrix} L_{11} & L_{12} & L_{13} \\ L_{12} & L_{22} & L_{23} \\ L_{13} & L_{23} & L_{33} \end{pmatrix} \begin{pmatrix} \delta\mu/T \\ \delta T/T^2 \\ \delta T_S/T^2 \end{pmatrix} . \tag{20}$$

The Casimir-Onsager relations $L_{ij} = L_{ji}$ for $i \neq j$ are valid in the absence of time-reversal symmetry breaking. In Ref. [21], we have discussed several possibilities offered by this setup when $\delta T_S \neq 0$, in terms of energy harvesting and cooling. Let us focus on the case where the NW is deposited on a hoter substrate without bias and temperature difference between the source and the drain ($\delta\mu = \delta T = 0$ while $\delta T_S > 0$). If the particle-hole symmetry and the left-right inversion symmetry are broken, the heat provided by the phonons can be exploited to produce electrical work. Let us consider a model where the NW localized states are uniformly distributed in space and energy within a band $[-2\epsilon, 2\epsilon]$ with a constant DOS $\nu = 1/(4\epsilon)$ and an energy independent localisation length $\xi = 4$. We have solved the corresponding RRN for an ensemble of M parallel NWs with asymetric elastic couplings to the electronics reservoirs. In

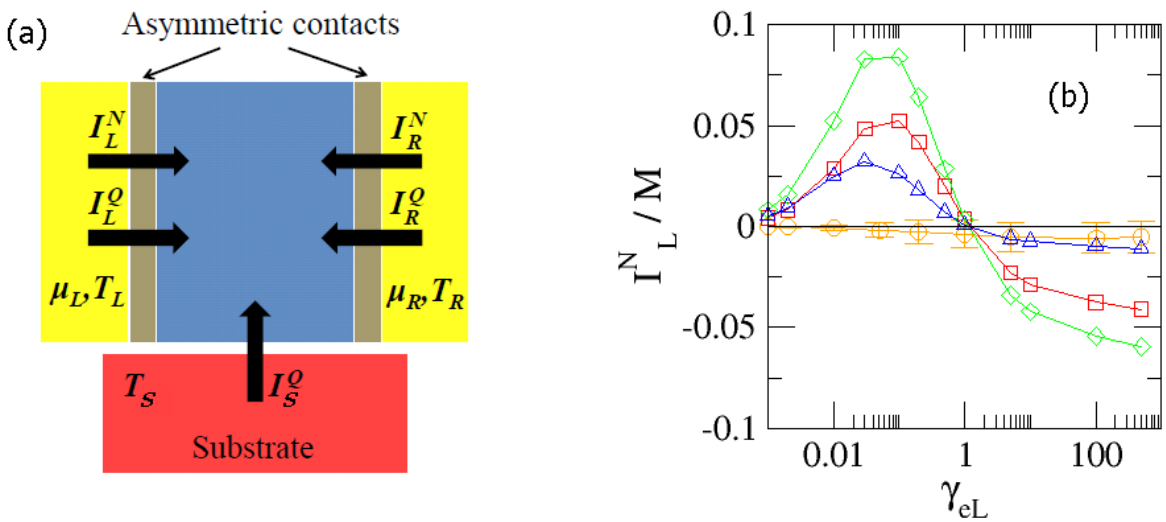

Figure 5: *(**a**): Scheme of the three-terminal setup corresponding to activated thermoelectric transport for a NW deposited on a substrate. The NW (blue) is connected to two electronic electrodes (yellow) L (the source) and R (the drain) via asymetric contacts. The electrodes are at equilibrium (electrochemical potentials μ_L, μ_R, and temperatures T_L, T_R). The insulating substrate (red) provides a phonon bath of temperature T_S. (**b**): Ratchet effect powered by $\delta T_S = 10^{-3}\,\epsilon$ when $\delta T = \delta\mu = 0$. For various values of V_g ($V_g/\epsilon = 0$ (○), 0.5 (□), 1 (◇) and 2.5 (△)), the average particle currents I_L^N/M (in unit of $10^5\epsilon/\hbar$) of an array of $M = 2.10^5$ parallel NWs is given as one varies γ_{eL} (elastic coupling to the source), keeping the same value $\gamma_{eR} = \epsilon/\hbar$ for the elastic coupling to the drain. $I_L^N/M \neq 0$, unless $V_g = 0$ (particle-hole symmetry) or $\gamma_{eL} = \gamma_{eR}$ (inversion symmetry).*

average over an ensemble of M NWs, particle-hole symmetry is broken if the Fermi potential $E_F \equiv 0$ does not coincide with the NW band centre ($V_g \neq 0$), and inversion symmetry is broken by taking different elastic coupling constants in Eq. (16) ($\gamma_{e,L} \neq \gamma_{e,R}$). Fig. 5 (**b**) gives the average particle current I_L^N/M between the source and the drain as a function of $\gamma_{e,L}$ when $\gamma_{e,R} = 1$ (in units of $\epsilon/\hbar$). I_L^N/M was induced by a temperature difference $\delta T_S = 10^{-3}\epsilon$ between the substrate and a deposited array of $M = 2.10^5$ parallel NWs. One can see that $I_L^N \approx 0$ at the band centre ($V_g = 0$) and when $\gamma_{e,L} = \gamma_{e,R}$, while $I_L^N \neq 0$ otherwise. Other ways of breaking inversion symmetry which give rise to even larger currents I_L^N are discussed in Ref. [21].

In summary, we have shown that arrays of 1D MOSFETs have good thermoelectric performances, notably when the electrochemical potential is in the vicinity of the NW band edges. They could be used for converting waste heat into useful electrical power and for cooling hot spots in microprocessors. Moreover, ratchet effects open interesting perspectives when electrical transport in the NWs can be activated by the phonons of the substrate. These thermoelectric devices use standard Si-based semi-conductor technology, which is cheap, non-toxic and widely developed in microelectronics.

References

[1] E. Pop, S. Sinha and K. Goodson, Heat Generation and Transport in Nanometer-Scale Transistors, Proceedings of the IEEE. 94 (2006) 1587. DOI: 10.1109/jPROC.2006.879794

[2] A. F. Ioffe, Semiconductor thermoelements, and thermoelectric cooling, Infosearch Limited, 1957.

[3] H. J. Goldsmid, Introduction to thermoelectricity, Springer-Verlag, 2010.

[4] A. I. Hochbaum, R. Chen, R. D. Delgado, W. Liang, E. C. Garnett, M. Najarian, A. Majumdar and P. Yang, Enhanced thermoelectric performance of rough silicon nanowires, Nature, 451, (2008) 163. DOI: 10.1038/nature06381.

[5] W. Poirier, D. Mailly and M. Sanquer, Tunneling and interferences in very small GaAs metal-semiconductor field-effect transistors, Phys. Rev B 59, 16 (1999) 10 856.

[6] C. Thelander, P. Agarwal, S. Brongersma, J. Eymery, L. F. Feiner, A. Forchel, M. Scheffler, W. Riess, B. J. Ohlsson, U. Gsele and L. Samuelson, Nanowire Based One-Dimensional Electronics. MaterialsToday 9 (10) (2006) 28-35.

[7] Y. U. Brovman, J. P. Small, Y. Hu, Y. Fang, C. M. Lieber and P. Kim, Electric field effect thermoelectric transport in individual silicon and germanium/silicon nanowires, J. Appl. Phys. 119 (2016) 234304. DOI: 10.1063/1.4953818.

[8] R. Bosisio, G. Fleury and J.-L. Pichard, Gate-modulated thermopower in disordered nanowires: I. Low temperature coherent regime, New J. Phys. 16 (2014) 035004. DOI: 10.1088/1367-2630/16/3/035004.

[9] B. Derrida and E. Gardner, Lyapunov exponent of the one dimensional Anderson model: weak disorder expansion. J. Phys. France 45 (1984) 1283.

[10] S. A. van Langen, P. G. Silvestrov and C. W. J. Beenakker, Thermopower of single-channel disordered and chaotic conductors, Supperlattices and Microstructures, 23 (1998) 691.

[11] R. Bosisio, C. Gorini, G. Fleury and J.-L. Pichard, Gate-modulated thermopower in disordered nanowires: II. Variable-range hopping regime, New J. Phys. 16, (2014) 095005. DOI: 10.1088/1367-2630/16/9/095005

[12] N. F. Mott and E. A. Davies, Electronic Processes in Non Crystalline Materials, 2nd edn (1979) (Oxford: Clarendon).

[13] J. Kurkijarvi, Hopping conductivity in one dimension, Phys. Rev B 8 (1973) 922.

[14] M. E. Raikh and M. E. Ruzin, Fluctuations of the hopping conductance in one dimensional systems, Sov. Phys. JETP 68 (1989) 642.

[15] , J. H. Yiang, O. Entin-Wohlman and Y. Imry, Thermoelectric three-terminal hopping transport through one-dimensional nanosystems, Phys. Rev. B 85 (2012) 075412.

[16] J. H. Yiang, O. Entin-Wohlman and Y. Imry, Hopping thermoelectric transport in finite systems: Boundary effects, Phys. Rev. B 87 (2013) 205420.

[17] Impurity conduction at low concentrations A. Miller and E. Abrahams, Phys. Rev. 120 (1960) 745.

[18] V. Ambegaokar, B. Halperin and J. Langer, Hopping conductivity in disordered systems, Phys. Rev. B 4 (1971) 2612.

[19] R. Bosisio, C. Gorini, G. Fleury and J.-L. Pichard, Using Activated Transport for Energy Harvesting and Hot-Spot Cooling, Phys. Rev. Applied 3 (2015) 054002. DOI: 10.1103/PhysRevApplied.3.054002

[20] R. Bosisio, C. Gorini, G. Fleury and J.-L. Pichard, Absorbing/emitting phonons with one dimensional MOSFETs, Physica E, 74 (2015) 340.
DOI: 10.1016/j.physe2015.07012

[21] R. Bosisio, G. Fleury, J.-L. Pichard and C. Gorini, Nanowire-based thermoelectric ratchet in the hopping regime, Phys. Rev. B 93, (2016) 165404. DOI: 10.1103/PhysRevB.93.165404